ACTIVE AND REACTIVE POWER CONTROL OF DFIG WIND   TURBINE WITH ENERGY STORAGE

Shaik Mohammad bilal

QUBA college of engineering, Nellore, Andhra pradesh, India

---***---

Abstract- Wind turbine generators (WTGs) are usually controlled to generate maximum electrical power from wind under normal wind conditions. With the increasing penetration of wind power into electric power grids, energy storage devices will be required to dynamically match the intermittency of wind energy. To meet the requirements of frequency and active power regulation, energy storage devices will be required to dynamically match the intermittency of wind energy. A novel two layer constant-power control scheme for a wind farm equipped with doubly-fed induction generator (DFIG) wind turbines. Each DFIG wind turbine is equipped with a super capacitor energy storage system (ESS) and is controlled by the low-layer WTG controllers and coordinated by a high-layer wind-farm supervisory controller (WFSC). The WFSC generates the active-power references for the low-layer WTG controllers according to the active-power demand from the grid operator; the low- layer WTG controllers then regulate each DFIG wind turbine to generate the desired amount of active power, where the deviations between the available wind energy input and desired active power output are compensated by the ESS. Simulation studies are carried out in mat lab on a wind farm equipped with dfig wind turbines to verify the effectiveness of the proposed control scheme

Index Terms—CONSTANT POWER CONTROL (CPC), DOUBLY FED INDUCTION GENERATOR (DFIG), ENERGY STORAGE, WIND FARM SUPERVISORY CONTROLLER(WFSC).

1. INTRODUCTION

WIND TURBINE generators (WTGs) are usually controlled to generate maximum electrical power fromwind under normal wind conditions. However, because of the variations of the wind speed, the generated electrical power of a WTG is usually fluctuated. Currently, wind energy only provides about 1%–2% of the world's electricity supply. At such penetration level, it is not necessary to require WTGs to participate in automatic generation control, unit commitment, or frequency regulation. However, it is reasonable to expect that wind power will be capable of becoming a major contributor to the nation's and world's electricity supply over the next three decades. For instance, the European Wind Energy Association has set a target to satisfy more than 22% of European electricity demand with wind power by 2030 [1]. In the U.S., according to a report[2] by the Department of Energy, it is feasible to supply 20% of the nation's electricity from wind by 2030. At such high levels of penetration, it will become necessary to require WTGs to supply a desired amount of active power to participate in automatic generation control or frequency regulation of the grid [3]. However, the intermittency of wind resources can cause high rates of change (ramps) in power generation [4], which is a critical issue for balancing power systems. Moreover, to optimize the economic performance of power systems with high penetrations of wind power, it would be desired to require WTGs to participate in unit commitment, economic dispatch, or electricity market operation [5]. In practice, short-term wind power prediction [6] is carried out to help WTGs provide these functions. However, even using the state-of-the-art methods, prediction errors are present [5]. Under these conditions, the replacement power is supported by reserves, which, however, can be more expensive than base electricity prices [7].To enable WTGs to effectively participate in frequency and active power regulation, unit commitment, economic dispatch, and electricity market operation, energy storage devices will be required to dynamically match the intermittency of wind energy. In [8], the authors investigated and compared different feasible electric energy storage technologies for intermittent renewable energy generation, such as wind power. Currently, pumped water and compressed air are the most commonlyused energy storage technologies for power grids due to their low capital costs [9]. However, these two technologies are heavily dependent on geographical location with relatively low round-trip efficiency. Compared with their peers, batteries and super capacitors are more efficient, have a quicker response to demand variations, and are easy to develop and ubiquitously deployable. Compared to batteries, super capacitors have a higher power density, higher round-trip efficiency, longer cycle life,and lower capital cost per cycle [10].
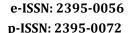
Fig. 1.1 Configuration of a DFIG wind turbine equipped with a super capacitor 9ESS connected to a power grid

Therefore, super capacitors are a good candidate for short-term (i.e., seconds to minutes) energy storage that enables WTGs to provide the function of frequency regulation and effectively participate in unit commitment

and electricity market operation. The use of super capacitors[10] or batteries [11]–[13] as energy storage devices forWTGs has been studied by some researchers. However, these studies only focused on control and operation of individual WTGs and did not investigate the issues of WTGs to participate in grid regulation. This paper proposes a novel two-layer constant power control(CPC) scheme for a wind farm equipped with doubly fed induction generator (DFIG) wind turbines [14], where each WTG is equipped with a super capacitor energy storage system(ESS). The CPC consists of a high-layer wind farm supervisory controller (WFSC) and low-layer WTG controllers. The high layer WFSC generates the active power references for the low layer WTG controllers of each DFIG wind turbine according to the active power demand from the grid operator. The low-layer WTG controllers then regulate each DFIG wind turbine to generate the desired amount of active power, where the deviations between the available wind energy input and desired active power output are compensated by the ESS. Simulation studies are carried out in PSCAD/EMTDC for a wind farm equipped with 15 DFIG wind turbines to verify the effectiveness of the proposed control scheme.

2. DFIG WIND TURBINE WITH ENERGY STORAGE

The low-speed wind turbine drives a high-speed DFIG through a gearbox. The DFIG is a wound-rotor induction machine. It is connected to the power grid at both stator and rotor terminals. The stator is directly connected to the grid, while the rotor is fed through a variable-frequency converter, which consists of a rotor-side converter (RSC) and a grid-side converter (GSC) connected back to back through a dc link and usually has a rating of a fraction (25%–30%) of the DFIG nominal power. As a consequence, the WTG can operate with the rotational speed in a range of ±25%–30% around the synchronous speed, and its active and reactive powers can be controlled independently. In this paper, an ESS consisting of a super capacitor bank and a two-quadrant dc/dc converter is connected to the dc link of the DFIG converters. The ESS serves as either a source or a sink of active power and therefore contributes to control the generated active power of the WTG. The value of the capacitance of the super capacitor bank can be determined by

Cess $= 2P_nT/V^2_{sc}$ (1)

Where Cess is in farads, $P_n$is the rated power of the DFIG in watts,

VSC is the rated voltage of the super capacitor bank in volts, and T is the desired time period in seconds that the ESS can supply/store energy at the rated power (P_n) of the DFIG.

The use of an ESS in each WTG rather than a large single central ESS for the entire wind farm is based on two reasons first, this arrangement has a high reliability because the failure of a single ESS unit does not affect the ESS units in other WTGs. Second, the use of an ESS in each WTG can reinforce the dc bus of the DFIG converters during transients, thereby enhancing the low-voltage ride through capability of the WTG [10].

3. CONTROL OF INDIVIDUAL DFIG WIND TURBINE

The control system of each individual DFIG wind turbine generally consists of two parts: 1) the electrical control of the DFIG and 2) the mechanical control of the wind turbine blade pitch angle [14], [15] and yaw system. Control of the DFIG is achieved by controlling the RSC, the GSC, and the ESS. The control objective of the RSC is to regulate the stator-side active power Ps and reactive power Qs independently. The control objective of the GSC is to maintain the dc-link voltage Vdc constant and to regulate the reactive power Qg that the GSC exchanges with the grid. The control objective of the ESS is to regulate the active power Pg that the GSC exchanges with the grid. In this paper, the mechanical control of the wind turbine blade pitch angle is similar to that in [15].

A. Control of the RSC

Fig. 2 shows the overall vector control scheme of the RSC, in which the independent control of the stator active power Ps and reactive power Qs is achieved by means of rotor current regulation in a stator-flux-oriented synchronously rotating reference frame [16]. Therefore, the overall RSC control scheme consists of two cascaded control loops. The outer control loop regulates the stator active and reactive powers independently, which generates the reference signals idr and iqr of the d- and q-axis current components, respectively, for the inner-loop currentregulation. The outputs of the two current controllers arecompensated by the corresponding cross-coupling terms $vdr0$ and $vqr0$ [14], respectively, to form the total voltage signals vdr and vqr.
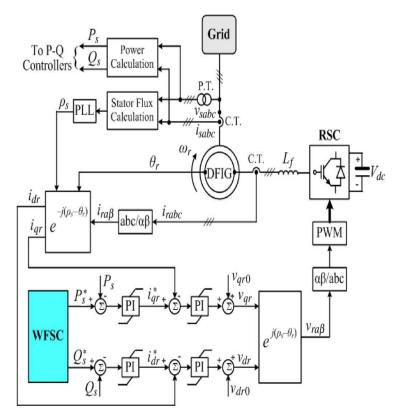

Fig.3.1 Overall vector control scheme of the RSC.

They are then used by the pulse width modulation(PWM) module to generate the gate control signals to drive theRSC. The reference signals of the outer-loop power controllersare generated by the high-layer WFSC.
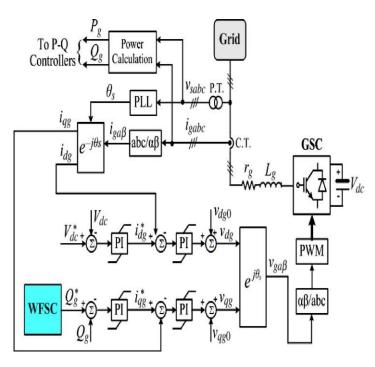
B.   Control of the GSC

Fig. 3.2. Overall vector control scheme of the GSC.

Fig. 3.2 shows the overall vector control scheme of the GSC, in which the control of the dc-link voltage V_{dc} and the reactive power Q_g exchanged between the GSC and the grid is achieved by means of current regulation in a synchronously rotating reference frame [16]. Again, the overall GSC control scheme consists of two cascaded control loops. The outer control loop regulates the dc-link voltage V_{dc} and the reactive power Q_g, respectively, which generates the reference signals i_{dg} and i_{qg} of the d- and q-axis current components, respectively, for the inner-loop current regulation. The outputs of the two current controllers are compensated by the corresponding cross coupling terms $v_{dg}0$ and $v_{qg}0$ [14], respectively, to form the total voltage signals v_{dg} and v_{qg}. They are then used by the PWM module to generate the gate control signals to drive the GSC. The reference signal of the outer-loop reactive power controller is generated by the high-layer WFSC.
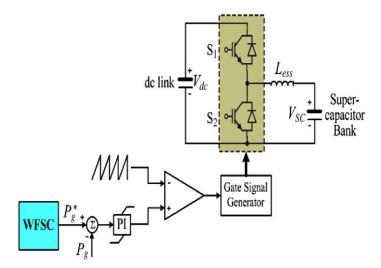

Fig. 3.3.Configuration and control of the ESS.

Fig. 3.3 shows the configuration and control of the ESS. The ESS consists of a super capacitor bank and a two-quadrant dc/dc converter connected to the dc link of the DFIG. The dc/dc converter contains two insulated-gate bipolar transistor (IGBT) switches S1 and S2. Their duty ratios are controlled to regulate the active power Pg that the GSC exchanges with the grid. In this configuration, the dc/dc converter can operate in two different modes, i.e., buck or boost mode, depending on the converter operates in the boost mode; if S2 is open, the dc/dc converter operates in the buck mode. The duty ratio $D1$ of S1 in the buck mode can be approximately expressed as

$$D1 = V_{sc}/V_{dc} \quad (2)$$

and the duty ratio $D2$ of S2 in the boost mode is

$$D2 = 1 - D1.$$

In this paper, the nominal dc voltage ratio $V_{SC,n}/V_{dc,n}$ is 0.5, where V_{SC},n and $V_{dc,n}$ are the nominal voltages of the super capacitor bank and the DFIG dc link, respectively. Therefore, the nominal duty ratio $D1,n$ of S1 is 0.5. The operating modes and duty ratios $D1$ and $D2$ of the dc/dcconverter are controlled depending on the relationship between the active powers Pr of the RSC and Pg of the GSC. If Pr is greater than Pg, the converter is in buck mode and $D1$ is controlled, such that the super capacitor bank serves as a sink to absorb active power, which results in the increase of its voltage VSC. On the contrary, if Pg is greater than Pr, the converter is inboost mode and $D2$ is controlled, such that the super capacitor bank serves as a source to supply active power, which results in the decrease of its voltage VSC. Therefore, by controlling the operating modes and duty ratios of the dc/dc converter, the ESS serves as either a source or a sink of active power to control the generated active power of the WTG. In Fig. 4, the reference signal Pg is generated by the high-layer WFSC. s of the two IGBT switches. If S1 is open, the dc/dc

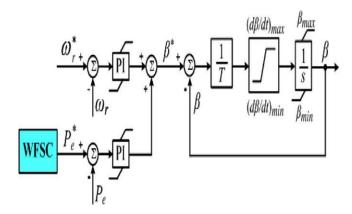### C.   Wind Turbine Blade Pitch Control

Fig. 3.4. Blade pitch control for the wind turbine.

Fig. 3.4 shows the blade pitch control for the wind turbine, where ωr and $Pe (= Ps + Pg)$ are the rotating speed and output active power of the DFIG, respectively. When the wind speed is below the rated value and the WTG is required to generate the maximum power, ωr and Pe are set at their reference values, and the blade pitch control is deactivated. When the wind speed is below the rated value, but the WTG is required to generate a constant power less than the maximum power, the active power controller may be activated, where the reference signal Pe is generated by the high-layer WFSC and Pe takes the actual measured value. The active power controller adjuststhe blade pitch angle to reduce the mechanical power that theturbine extracts from wind. This reduces the imbalance betweenthe turbine mechanical power and the DFIG output activepower, thereby reducing the mechanical stress in the WTGand stabilizing the WTG system. Finally, when the wind speed

increases above the rated value, both ωr and Pe take the actual measured values, and both the speed and active power controllers are activated to adjust the blade pitch angle.
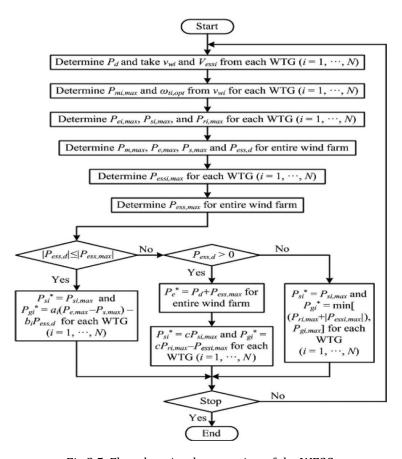
Fig.3.5. Flowchart implementation of the WFSC.

4. WIND FARM SUPERVISORY CONTROL

The objective of the WFSC is to generate the reference signals for the outer-loop power controllers of the RSC and GSC, the controller of the dc/dc converter, and the blade pitch controller of each WTG, according to the power demand from or the generation commitment to the grid operator. The implementation of the WFSC is described by the flowchart in Fig. 6,where$P_d$is the active power demand from or the generation commitment to the grid operator; v_{wi} and V_{essi} are the wind speed in meters per second and the voltage of the super capacitor bank measured from WTG i(i= 1, . . . , N), respectively; and N is the number of WTGs in the wind farm. Based on v_{wi}, the optimal rotational speed ω_{ti}, radians per second of the wind turbine can be determined, which is proportional to the wind speed v_{wi}at a certain pitch angle β_i

$$\omega_{ti,\mathrm{opt}}= k(\beta_i)v_{wi} \quad (3)$$

where$k$ is a constant at a certain value of β_i. Then, the maximum mechanical power $P_{mi,}$ max that the wind turbine extracts from the wind can be calculated by the well-known wind turbine aerodynamic characteristics

$$P_{mi,\max}=1/2\rho_iA_rv^3{}_{wi}C_{Pi}(\lambda_{i,\mathrm{opt}}, \beta_i) \quad (4)$$

where $\rho_i$is the air density in kilograms per cubic meter; A_r= $\pi R2$ is the area in square meters swept by the rotor blades, with R being the blade length in meters; and C_{Pi} is the power coefficient, which is a function of both tip-speed ratio λ_i and the blade pitch angle β_i, where λ_i is defined by

$$\lambda_i= \omega_{ti}R/v_{wi} \quad (5)$$

In (4), λi, the optimal tip-speed ratio when the wind turbine rotates with the optimal speed ωti, optat the wind speed vwi. Given Pmi, max, the maximum active power Pei,max generated by the WTG can be estimated by taking into account the power losses of the WTG [14]

$$P_{ei,\max}= P_{mi,\max}-P_{Li}= P_{si,\max}+ P_{ri,\max} \quad (6)$$

Where PLi is the total power losses of WTG i, which can be estimated by the method in [14]; Psi ,max and Pri,max are the maximum DFIG stator and rotor active powers of WTG i, respectively. In terms of the instantaneous variables in Fig. 1,the stator active power Ps can be written in a synchronously

Rotating dq reference frame [16] as follows:

$$P_s=3/2(v_{ds}i_{ds}+ v_{qs}i_{qs})$$

$$\approx 3/2[(\omega_s L_m(i_{qs}i_{dr}-i_{ds}i_{qr}) +r_s(i^2_{ds}+ i^2_{qs})] \quad (7)$$

where $vd\,s$and vqs are the d- and q-axis voltage components of the stator windings, respectively; ids and $iq\,s$are the stator d- and q-axis current components, respectively; idr and iqr are the rotor d- and q-axis current components, respectively; $\omega\,s$is the rotational speed of the synchronous reference frame; and rs and Lm are the stator resistance and mutual inductance, respectively. Similarly, the rotor active power is calculated by

$$P_r=3/2(v_{dr}i_{dr}+ v_{qr}i_{qr})$$

$$\approx 3/2[-s\omega_s L_m(i_{qs}i_{dr}-i_{ds}i_{qr}) +i^2_{dr}+ i^2_{qr}] \quad (8)$$

Where $vd\,r$and $vq\,r$are the d- and q-axis voltage components of the rotor windings, respectively; s is the slip of the DFIG defined by

$$s = (\omega_s-\omega_r)/\omega_s \quad (9)$$

where ωr is the DFIG rotor speed. (7) and (8) yield

$$s = -[P_r-3i^2_r r_r/P_s-3i^2_s r_s] \quad (10)$$

where $is =i2ds + i2qs/2$ and $ir=i2dr + i2qr/2$. If neglecting the stator copper loss $3i2srs$and rotor copper loss $3i2rr$ofthe DFIG, the relationship between the stator and rotor active powers can be approximated by

$$P_r= -sP_s. \quad (11)$$

Fig. 4.1. Flowchart of determination of $Pessi$,maxfor each WTG.

According to (6) and (10) [or (11)], Psi,max and Pri,max of each WTG can be determined. Then, the total maximum mechanical power Pm,max, DFIG output active power Pe,max, and statoractive power Ps,max of all WTGs in the wind farm can be calculated as

$$P_{m,max} = \Sigma P_{mi,max} \qquad (12)$$

$$Pe,max = \Sigma Pei,max \qquad (13)$$

$$Ps,max = \Sigma Psi,max \qquad (14)$$

In order to supply constant power Pd to the grid, the deviation $Pess,d$ between the demand/commitment Pd and the maximum generation Pe,max is the power that should be stored in or supplied from the ESSs of the WT

$$P_{ess,d} = P_{e,max} - P_d. (15)$$

On the other hand, the capability of each ESS to store or supply power depends on the capacitance C_{ess} and the voltage V_{essi} of the supercapacitor bank. During normal operation, V_{essi} must be maintained within the following range:

$$V_{i,min} < V_{essi} < V_{i,max} (16)$$

Where Vi,max and Vi,min are the maximum and minimum operating voltages of the supercapacitor bank, respectively. The maximum power $Pessi,max$ that can be exchanged between the supercapacitor bank and the DFIG dc link of WTG $i$can be determined by

$$P_{essi,max} = \pm C_{ess} V_{essi} \left| dV_{essi}/dt \right|_{max} (17)$$

Where $|dVessi/dt|max$ is the maximum rate of voltage variations of the supercapacitor bank, which is related to the current limits of the supercapacitor bank. In (17), the positive sign indicates storing energy, while the negative sign indicates supplying energy by the ESS. The calculation of $Pessi,max$ for each WTG is subjected to (16). Fig. 7 shows how to determine $Pessi,max$ for each WTG. If $Pess,d>0$, extra power needs to be stored in the ESSs. In this case, if $Vessi<Vi,max$, $Pessi,max$ is calculated by (17) and takes the positive sign; otherwise, the \ESS cannot store any power and $Pessi,max= 0$. On the contrary, if $Pess,d<0$, active power needs to be supplied from the ESSs. In this case, if $Vessi>Vi,min$, $Pessi,max$ is calculated by (17) and takes thenegative sign; otherwise, the ESS cannot supply any power and

$$Pessi,max = 0.$$

As shown in Fig. 6, once $Pessi,max$ of each WTG is determined, the total maximum power $Pess,max$ that can be exchanged between the supercapacitor bank and the DFIG dc link of all WTGs can be determined by

$$P_{ess,max} = \Sigma P_{essi,max}. (18)$$

Finally, depending on the relationship of $Pess,d$ and $Pess,max$, the reference signals Psi(see Fig. 2) and Pgi(see Fig. 4) of each WTG can be determined. Specifically, if $|Pess,d||Pess,max|$,Ps $i$and Pgi can be determined directly, as shown in Fig. 6,where the partition coefficients ai's are calculated by

$$a_i = P_{ri,max}/P_{e,max} - P_{s,max} (19)$$

and the partition coefficients bi's are calculated by

$$b_i = P_{essi,max}/P_{ess,max} (20)$$

The coefficients $ai$and bi have the following feature:

$$\Sigma a_i = 1 \qquad \Sigma b_i = 1. (21)$$

If $|Pess,d| > |Pess,max|$, depending on the sign of $Pess,d$, Psi and Pgi can be determined, as shown in Fig. 6. If $Pess,d$ is positive, the ESSs of the WTGs store active power, and the total active

power generated by all DFIGs is $P*e$, which is less than Pe,max. Therefore, a scaling factor c is defined as follows:

$$c = P^{*}{}_e P_{e,\max} \qquad (22)$$

and Psi and Pgi can be determined by using the scaling factor.

If $Pess,d$ is negative, the ESSs of the WTGs supply active power, the RSC of each WTG is controlled to generate the maximum stator active power Psi,max, and the ESS of each WTG is controlled to generate active power of Pgi, where Pgi,max is the maximum value of Pgi depending on the maximum power capacity of the GSC.

CPC scheme for the wind farm, where Pd is the active power demand from or commitment to the grid operator. In practice, the value of Pd should take into account the generation capability of the wind farm and should be subjected to the following limit:$Pd \leq Pe,\max$(23)

Where Pe,max is the average value of Pe,max over the period that Pd will be constant and the value of Pe,max during the period can be obtained from short-term wind power prediction [6]. This function allows the wind farm to be able to actively participate in automatic generation control, unit commitment, or frequency regulation of the grid, where the deviations between the available wind energy input and desired active power

output are compensated by the ESSs. Under the condition of (23) and the ESS of a WTG has been fully filled up, then the power reference of the blade pitch controller in Fig. 5 is set at Pd by the WFSC to adjust the pitch angle to reduce the WTG output active power to Pd. Moreover, the implementation of the WFSC (Fig. 6) subject to (23) ensures that the use of the ESS does not need to increase the rating of the RSC or the GSC.

The reactive power references of the RSC (Fig. 2) and GSC (Fig. 3) controllers can be determined by controlling the power factor (pf) or the voltage ($VPCC$) at the point of common coupling (PCC) of the wind farm at the desired value or to supply a desired amount of reactive power as required by the grid operator. However, these issues are not in the scope of this paper. In this paper, the reactive power references of all RSC and GSC controllers are simply set as zero.

5. SIMULATION RESULTS

Simulation studies are carried out for a wind farm with DFIG wind turbines verify the effectiveness of the proposed control scheme under various operating conditions. Each DFIG wind turbine has a 3.6-MW power capacity [14], [15]. The total power capacity of wind farm is 54 MW. Each DFIG wind turbine is connected to the internal network of the wind farm through a 4.16/34.5-kV voltage step-up transformer. The high-voltage terminals of all transformers in the wind farm are connected by 34.5-kV power cables to form the internal network of the wind farm. The entire wind farm is connected to the utility power grid through a 34.5/138-kV voltage step-up transformer at PCC to supply active and reactive powers of P and Q, respectively. In this paper, the power grid is represented by an infinite source. The ESS of each WTG is designed to continuously supply/store 20% of the DFIG rated power for approximately 60 s. Then, the total capacitance of the super capacitor bank can be obtained from (1). The parameters of the WTG, the ESS, and the power network are listed in the Appendix. Some typical results are shown and discussed in this section.

A. CPC During Variable Wind Speed Conditions

Fig. 5.1shows the wind speed profiles of WTG1 ($vw1$),WTG6($vw6$), and WTG11 ($vw11$). The wind speeds across the three WTGs vary in a range of ±3 m/s around their mean value of 12 m/s. The variations of wind speed cause fluctuations of the electrical quantities of the WTGs. As shown in Fig. 11, if the wind farm is not equipped with any energy storage devicesor the proposed CPC scheme, the wind speed variations in the

wind farm result in significant fluctuations of the total output active power at the PCC. The wind farm power output deviates significantly from the active power demand or commitment. In future electric power grids where the penetration of wind

power is high (e.g., 20%), such active power fluctuations can bring severe problems to grid operation. Fig. 12 compares the total output active power of the wind farm with the power demand from or commitment to the grid
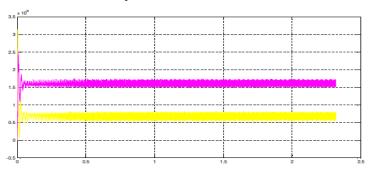

Fig.5.1active and reactive power of wind turbine

operator, where each WTG is equipped with an ESS as shown in Fig. 1. The ESS stores energy when the WTG generates more active power than the demand/commitment and supplies energy when the WTG generates less active power than the demand/commitment. The resulting output power of the wind farm is therefore controlled at a constant value as required by the grid operator. Fig. 13 shows the total stator active power Ps and the total

GSC active power $Pg$of all WTGs, as well as the total output active power P (measured at PCC) of the wind farm. Through the control of the proposed CPC scheme, the variations of the stator active power are exactly compensated by the variations of the GSC active power. Consequently, the total output active power of the wind farm is constant. However, the total output active power Pei of each individual WTG, which is the sum

of the stator active power Psi and the GSC active power Pgi, is usually not constant, as shown in Fig. 14 for WTG 1. Thedeviations between the RSC active power (Pri) and the GSCactive power (Pgi) of each WTG are stored in or supplied by the ESS ($Pessi$), as shown in Fig. 15 for WTG 1.
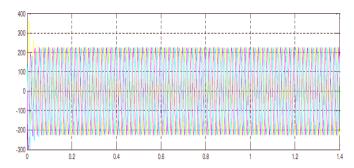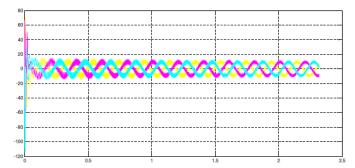

Fig.5.2 stator current of wind turbine

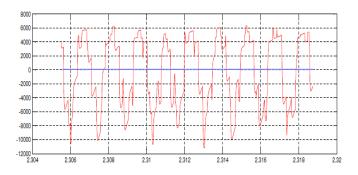Fig.5.5 rotor currents of wind turbine

Fig.5.6 stator voltages of wind turbine

B. Power Tracking During Step Changes in Demand/Commitment

Under the same wind conditions as in the previous tests, the power demand from or commitment to the grid operator is now step changed from time to time. The wind farm is controlled by the proposed CPC scheme to track the variations of the power demand. Fig. 17 shows the power tracking performance of the wind farm. The generated active power by the wind farm dynamically tracks the power demand/commitment with good precision. This power tracking capability cannot be achieved without using the ESSs or the proposed control scheme. Fig. 18 shows the total active power outputs of WTG1 and WTG5. Although the total output power of the wind farm is controlled to be constant during each time interval, as shown in Fig. 17, the total active power output of each individual WTG is not constant. Under the regulation of the proposed CPC scheme, including the blade pitch control, the output power of each WTG is always kept within its limits of 3.6 MW.
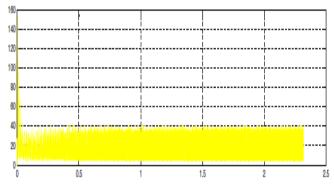

Fig.5.4 voltages of the supercapacitor bank

6. CONCLUSION

This paper has proposed a novel two-layer CPC scheme for a wind farm equipped with DFIG wind turbines. Each wind turbine is equipped with a supercapacitor-based ESS, which is connected to the dc link of the DFIG through a two-quadrant dc/dc converter. The ESS serves as either a source or a sink of active power to control the generated active power of the DFIG wind turbine. Each individual DFIG wind turbine and its ESS are controlled by low-layer WTG controllers, which are coordinated by a high-layer WFSC to generate constant active power as required by or committed to the grid operator. Simulation studies have been carried out for a wind farm equipped with 15 DFIG wind turbines to verify the effectiveness of the proposed CPC scheme. Results have shown that the proposed CPC scheme enabled the wind farm to effectively participate in unit commitment and active power and frequency regulations of the grid. The proposed system and control scheme provides a solution to help achieve high levels of penetration of wind power into electric power grids.

7. REFERENCES

[1] "Focus on 2030: EWEA aims for 22% of Europe's electricity by 2030,"*Wind Directions*, pp. 25–34, Nov./Dec. 2006.

[2] 20% Wind Energy By 2030: Increasing Wind Energy's Contribution to U.S. Electricity Supply, U.S. Department of Energy, Jul. 2008.

[3] W. Qiao and R. G. Harley, "Grid connection requirements and solutions for DFIG wind turbines," in *Proc. IEEE Energy Conf.*, Atlanta, GA,Nov. 17–18, 2008, pp. 1–8.

[4] Wind Generation & Total Load in the BPA Balancing Authority: DOE Bonneville Power Administration, U.S. Department of Energy. [Online].Available: http://www.transmission.bpa.gov/business/operations/Wind/default.aspx.

[5] R. Piwko, D. Osborn, R. Gramlich, G. Jordan, D. Hawkins, and K. Porter, "Wind energy delivery issues: Transmission planning and competitive electricity market operation," *IEEE Power Energy Mag.*, vol. 3, no. 6,pp. 47–56, Nov./Dec. 2005.

[6] L. Landberg, G. Giebel, H. A. Nielsen, T. Nielsen, and H. Madsen, "Shorttermprediction—An overview," *Wind Energy*, vol. 6, no. 3, pp. 273–280, Jul./Sep. 2003.

[7] M. Milligan, B. Kirby, R. Gramlich, and M. Goggin, Impact of Electric Industry Structure on High Wind Peneration Potential, Nat. Renewable Energy Lab., Golden, CO, Tech. Rep. NREL/TP-550-46273. [Online]. Available: http://www.nrel.gov/docs/fy09osti/46273.pdf

[8] J. P. Barton and D. G. Infield, "Energy storage and its use with intermittent renewable energy," *IEEE Trans. Energy Convers.*, vol. 19, no. 2, pp. 441–448, Jun. 2004.

[9] D. Rastler, "Electric energy storage, an essential asset to the electric enterprise:Barriers and RD&D needs," *California Energy Commission StaffWorkshop Energy Storage Technol., Policies Needed Support California's RPS Goals 2020*, Sacramento, CA, Apr. 2, 2009.

[10] C. Abbey and G. Joos, "Supercapacitor energy storage for wind energy applications," *IEEE Trans. Ind. Appl.*, vol. 43, no. 3, pp. 769–776, May/Jun. 2007.

[11] B. S. Borowy and Z. M. Salameh, "Dynamic response of a stand-alone wind energy conversion system with battery energy storage to wind gust,"*IEEE Trans. Energy Convers.*, vol. 12, no. 1, pp. 73–78, Mar. 1997.

[12] M.-S. Lu, C.-L.Chang, W.-J. Lee, and L. Wang, "Combining the wind power generation system with energy storage equipments," *IEEE Trans.Ind. Appl.*, vol. 45, no. 6, pp. 2109–2115, Nov./Dec. 2009.

[13] A. Yazdani, "Islanded operation of a doubly-fed induction generator (DFIG) wind-power system with integrated energy storage," in *Proc.IEEE Canada Elect. Power Conf.*, Montreal, QC, Canada, Oct. 25–26, 2007, pp. 153–159.

[14] W. Qiao, W. Zhou, J. M. Aller, and R. G. Harley, "Wind speed estimation based sensorless output maximization control for a wind turbine driving a DFIG," *IEEE Trans. Power Electron.*, vol. 23, no. 3, pp. 1156–1169, May 2008.

[15] W. Qiao, G. K. Venayagamoorthy, and R. G. Harley, "Real-time implementation of a STATCOM on a wind farm equipped with doubly fed induction generators," *IEEE Trans. Ind. Appl.*, vol. 45, no. 1, pp. 98–107, Jan./Feb. 2009.

[16] D. W. Novotny and T. A. Lipo, *Vector Control and Dynamics of AC Drives*. Oxford, U.K.: Oxford Univ. Press, 2000.